Hydrodynamics of lyotropic smectics : a dynamic light scattering study of dilute lamellar phases

F. Nallet, D. Roux, Jacques Prost

J. Phys. France **50** (1989) 3147-3165 15 OCTOBRE **1989,** PAGE 3147

Classification
Physics Abstracts
61.30 — 62.90 — 82.70D

Hydrodynamics of lyotropic smectics : a dynamic light scattering study of dilute lamellar phases

F. Nallet ([1]), D. Roux ([1]) and J. Prost ([2])

([1]) Centre de recherche Paul-Pascal, Domaine universitaire, 33405 Talence Cedex, France
([2]) Ecole supérieure de physique et de chimie industrielles, 10 rue Vauquelin, 75231 Paris Cedex 05, France

(*Reçu le 19 mai 1989, accepté le 7 juillet 1989*)

Résumé. — Des mesures de diffusion dynamique de la lumière ont été effectuées sur des échantillons orientés de phases smectiques lyotropes diluées. L'hydrodynamique des smectiques A binaires est utilisée pour décrire le spectre des fluctuations dans les échantillons. Le seul mode hydrodynamique expérimentalement accessible est le mode *barocline* (ainsi que son cas limite : le mode d'ondulation), dont l'origine est le couplage entre fluctuations de concentration et fluctuations de déplacement des couches. Sa relation de dispersion anisotrope est fonction notamment de deux constantes élastiques : le module de compression des couches (à potentiel chimique constant) $\bar{B}$; le module de courbure des couches K. L'étude de la flexibilité des membranes (K) et des interactions intermembranaires ($\bar{B}$) a lieu sur une droite de dilution le long de laquelle le pas du smectique varie de 4 à 35 nm. Les résultats confortent la description en termes de membranes flexibles (flexibilité proche de $k_B T$) soumises à l'interaction stérique de Helfrich.

Abstract. — Dynamic light scattering measurements on oriented samples of dilute lyotropic smectics have been performed. The hydrodynamics of two-component smectics A is applied to describe the fluctuation spectrum in our multicomponent samples. The experimentally relevant hydrodynamic mode is the *undulation/baroclinic* mode, which arises from the coupling between concentration and layer displacement fluctuations. Two elastic constants, the layer compressibility modulus (at constant chemical potential) $\bar{B}$ and the bending modulus K, are extracted from its anisotropic dispersion relation. Membrane flexibility (K) and intermembrane interactions ($\bar{B}$) have been studied along a dilution line, with smectic repeating distances in the range 4-35 nm. The results support the view of flexible membranes (flexibility of the order of $k_B T$) interacting by means of Helfrich's steric interaction.

1. Introduction.

Lyotropic smectics, as hinted by the etymology of their name, are liquid crystalline phases obtained when soap (more generally an amphiphilic compound) dissolves in water. They are therefore multicomponent systems whereas thermotropic smectics can be a single component. Owing to the hydrophobic effect, surfactant molecules in solution aggregate in various structures among which bilayers (membranes) are often encountered. When stacked in

periodic layers, these membranes lead to a smectic A phase [1]. Such a structure allows a convenient study of their physical properties such as flexibility and interactions. Indeed, as we explain later, flexibility can be traced from the smectic bending modulus K and interactions from the compressibility modulus $\bar{B}$.

Even if the smectic order is most often found in the concentrated regime, in some cases it may still exist at high dilution (low amphiphilic content) [2-4]. These dilute lamellar phases are of special interest : they are unique example of colloidal smectics and one illustration of phases of surfaces. In the dilute range, smectic repeating distances can reach several thousands of angstroms [5-7]. As for regular colloids, the large length scales simplify the description of the physics of these phases : interactions are no longer dominated by microscopic molecular forces and continuous descriptions are more safely applicable. Thus the possibility of changing continuously the repeating distance d (from 10 Å to more than 1 000 Å) is specially useful in the study of interacting membranes. Besides, owing to their large flexibility, the membrane conformations and physical properties are strongly affected by thermal fluctuations [8-11].

Recently, much effort has been devoted to the measurement of elastic properties of dilute lamellar phases. Using different techniques such as EPR [12], response under mechanical constraint [13] and high resolution X-ray scattering [14, 15] informations on flexibility and membrane interactions have been obtained. One of the most remarkable results is the experimental evidence for repulsive undulation forces which have been proposed some years ago as a possible mechanism for membranes to interact [8]. These forces are entropic in origin : they come from the hindrance to undulations on account of the steric short distance repulsion between membranes. They arise on the same physical grounds as the pressure of a polymer constrained between two hard walls [16] or the steric repulsion between wandering lines of defects in the two-dimensional commensurate-incommensurate phase transition [17]. The reason why these repulsive interactions are strong enough to overcome the Van der Waals attraction is the large flexibility of the membranes : indeed, in these systems, the *membrane* bending constant κ is of the order of the thermal energy $k_B T$.

Light scattering is a particularly convenient way for measuring elastic constants of liquid crystals. Both static and dynamic measurements give, in principle, an access to the elastic moduli. Static measurements, although giving direct information, are difficult to achieve experimentally ; on the other hand dynamic ones, which are easier, require a hydrodynamic model to interpret the results. The hydrodynamic of the one-component smectic A has been worked out by de Gennes [18] and, in a more general context, by Martin *et al.* (MPP) [19] ; light scattering experiments have been performed confirming the validity of the approach [20-22]. The case of two-component smectics A has been explicitly studied by Brochard and de Gennes [23] but less investigated experimentally [24-26].

We present in this paper an extensive study of the hydrodynamics and light scattering of multicomponent lamellar phases. In part 2 we recall briefly the elasticity of two-component smectics A. Then, in the following part, we reformulate and generalize the hydrodynamics of two-component smectics A using the MPP framework. In a fourth part we describe the experiments we have performed on a typical dilute lamellar phase, previously studied with other techniques [13, 14]. In part 5 we give experimental results that permit us to measure the two elastic moduli $\bar{B}$ and K independently. The last part is devoted to an interpretation of the dilution behaviour of the elastic constants in terms of flexibility and interactions between membranes.

2. Elasticity of two-component smectic A.

The free energy density f of two-component, isothermal and incompressible smectics A, up to

second order in layer displacement u and concentration fluctuations δc (mass fraction), is [23] :

$$f = \frac{1}{2} B(\partial_z u)^2 + \frac{1}{2} K(\nabla_\perp^2 u)^2 + \frac{1}{2\chi} \delta c^2 + C_c \, \delta c \, \partial_z u \tag{1}$$

with B defined as the layer compression modulus (at constant concentration), K as the bending modulus, χ as the osmotic compressibility (at constant layer spacing) and C_c as the coupling constant between layer displacement and concentration fluctuations.

Of particular significance is the combination $\bar{B} = B - C_c^2 \chi$, which is the layer compressibility modulus at *constant chemical potential.* This elastic constant $\bar{B}$ may be related to the interactions between membranes, as we now explain. Let us describe the microscopic structure as a stack of surfactant bilayers of thickness δ and repeating distance d (Fig. 1). On geometrical grounds, the surfactant concentration (mass fraction) is expressed as :

$$c = \frac{m_S}{\rho v_S} \frac{\delta}{d} \tag{2}$$

where m_S is the molecular mass of the surfactant, v_S its molecular volume and ρ the total mass density. If we assume that both the solvent and the surfactant are incompressible

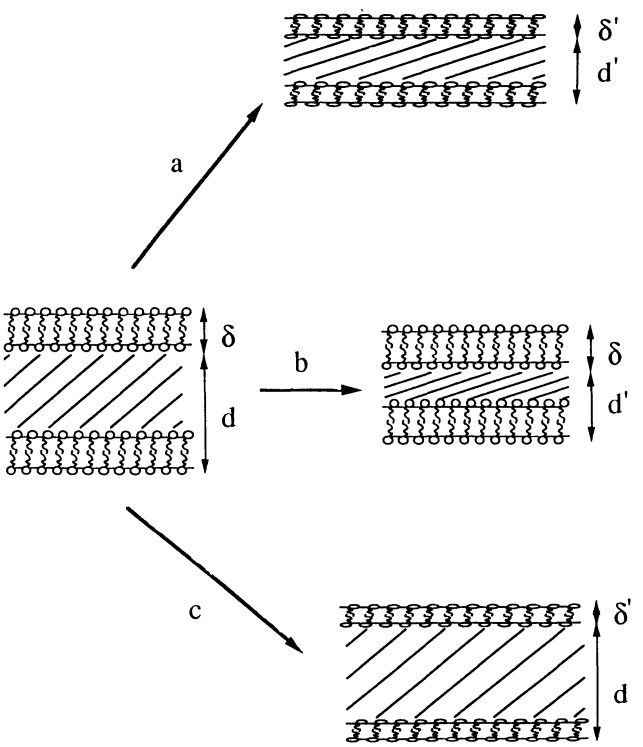

Fig. 1. — Schematic representations of unstrained and deformed states of a lyotropic smectic A with membrane thickness δ and repeating distance d. Layer compression at constant surfactant concentration (a), layer compression at constant membrane thickness (b) and membrane compression at constant layer thickness (c) are displayed. The elastic stresses are controlled respectively by B(a), $\bar{B}$(b) (in the appropriate limit) and χ(c).

v_S and ρ are constants. The equilibrium values for δ and d at a given concentration c result from a competition between two antagonist trends : the bilayer thickness δ tends to be close to some value δ_0, which would be the thickness of an isolated membrane ; on account of the membrane-membrane interactions the repeating distance d_0, resulting from equation (2) ($d_0 = m_S\,\delta_0/\rho v_S\,c$), is not the optimum one. A simplified model for the energy (per unit volume) of the stack structure which features this competition is a sum of two terms :

$$f = \frac{1}{2}\,\varepsilon\,\frac{\rho c}{m_S}\left(\frac{\delta - \delta_0}{\delta_0}\right)^2 + \frac{V(d)}{d} \tag{3}$$

where ε is a characteristic surfactant energy, $\rho c/m_S$ the number density of surfactant and $V(d)$ the membrane-membrane interaction potential per unit area. The first term is written in the harmonic approximation, valid for small departures from the reference thickness δ_0.

The equilibrium repeating distance d_{eq} is the solution of the minimization equation :

$$\left(\frac{V(d)}{d}\right)' + \varepsilon\,\frac{\rho c}{m_S}\,\frac{d - d_0}{d_0^2} = 0 \tag{4}$$

and is close to d_0 at large dilution. Concentration and repeating distance fluctuations around equilibrium are described by a Taylor expansion of the free energy (Eq. (3)), up to second order :

$$f = f_{eq} + 1^{st}\text{ order terms} + \frac{1}{2}\left(\frac{\partial^2 f}{\partial d^2}\,(d - d_{eq})^2 + 2\,\frac{\partial^2 f}{\partial d\,\partial c}\,(d - d_{eq})\,\delta c + \frac{\partial^2 f}{\partial c^2}\,\delta c^2\right). \tag{5}$$

By comparison with equation (1) we identify :

$$\begin{aligned} B &= \left(\frac{V(d)}{d}\right)''\,d_{eq}^2 + U\,\frac{d_{eq}}{d_0} \\ \chi^{-1} &= \frac{U}{c^2}\left(\frac{3\,d_{eq}}{d_0} - 2\right) \\ C_c &= \frac{U}{c}\left(\frac{3\,d_{eq}}{d_0} - 2\right) \end{aligned} \tag{6}$$

with $U = \varepsilon\,\dfrac{\rho c}{m_S}\,\dfrac{d_{eq}}{d_0}$.

Using the definition $\bar{B} = B - C_c^2\,\chi$ and equations (4) and (6) we get the layer compression modulus at constant chemical potential :

$$\bar{B} = d_{eq}\,V''. \tag{7}$$

From equations (6) and (7) the difference between B and $\bar{B}$ and the importance of this last elastic constant is clear : the layer compression modulus *at constant concentration* B is related to both the intrinsic energy ε and the membrane-membrane interactions V, whereas the layer compression modulus *at constant chemical potential* $\bar{B}$ is characteristic of the interactions alone. At large dilution B is dominated by the bilayer thickness rigidity ($B \approx \varepsilon\rho c/m_S$) and we have $\bar{B} \ll B$. These properties are illustrated in figure 1, which features three basic elastic deformations of a lyotropic smectic A. Note that a compression at constant concentration,

which keeps δ/d constant, corresponds to both a diminution of the bilayer thickness and a decrease of the repeating distance [27].

The elastic constant $\bar{B}$ is the one which is most readily obtained in a *static* experiment, as is apparent on the expressions for the correlation functions :

$$\langle u(\mathbf{q})\, u(-\mathbf{q})\rangle = \frac{k_B T}{\bar{B} q_z^2 + K q_\perp^4} \equiv S_{uu} \tag{8a}$$

$$\langle \delta c(\mathbf{q})\, \delta c(-\mathbf{q})\rangle = \frac{k_B T \chi (B q_z^2 + K q_\perp^4)}{\bar{B} q_z^2 + K q_\perp^4} \equiv S_{cc} \tag{8b}$$

$$\langle u(\mathbf{q})\, \delta c(-\mathbf{q})\rangle = i \frac{k_B T C_c \chi q_z}{\bar{B} q_z^2 + K q_\perp^4} \equiv S_{uc} . \tag{8c}$$

In a light scattering experiment, by a proper choice of the polarizations, it is possible to measure separately the two correlation functions $\langle c(\mathbf{q})\, c(-\mathbf{q})\rangle$ and $\langle u(\mathbf{q})\, u(-\mathbf{q})\rangle$. Indeed, the dielectric tensor for a uniaxial medium is :

$$\varepsilon_{\alpha\beta} = \bar{\varepsilon}\delta_{\alpha\beta} + \Delta\varepsilon \left(n_\alpha n_\beta - \frac{1}{3}\delta_{\alpha\beta} \right) \tag{9}$$

where $\bar{\varepsilon}$ is the mean dielectric constant, $\Delta\varepsilon$ the dielectric anisotropy, $\delta_{\alpha\beta}$ the Kronecker symbol, and n_α the component along the α-axis of the director (optical axis) of the medium. In the case of a low birefringence ($\Delta\varepsilon \ll 1$), the intensity of the light scattered at a wave vector $\mathbf{q}$, for an incoming polarization $\mathbf{i}$ and an outgoing one $\mathbf{f}$, is proportional to :

$$I_{fi}(\mathbf{q}) = \left(\frac{\partial \bar{\varepsilon}}{\partial c} \right)^2 (\mathbf{f}\cdot\mathbf{i})^2 S_{cc}(\mathbf{q}) + \Delta\varepsilon^2 (f_z \mathbf{i}\cdot\mathbf{q}_\perp + i_z \mathbf{f}\cdot\mathbf{q}_\perp)^2 S_{uu}(\mathbf{q}) +$$

$$+ 2 \frac{\partial \bar{\varepsilon}}{\partial c} \Delta\varepsilon\, \mathbf{f}\cdot\mathbf{i} (f_z \mathbf{i}\cdot\mathbf{q}_\perp + i_z \mathbf{f}\cdot\mathbf{q}_\perp)\, \mathrm{Im}(S_{uc}(\mathbf{q})) \tag{10}$$

where S_{cc}, S_{uu} and S_{uc} are the correlation functions defined in equation (8).

An X-ray (or neutron) scattering experiment in the vicinity of the quasi-Bragg peak is a measurement of the shape of the total mass density autocorrelation function, which is related to $\langle u(\mathbf{q})\, u(-\mathbf{q})\rangle$ [28] ; on the other hand, the scattered intensity *at small angles* originates in surfactant concentration fluctuations [29], which should in principle be described by $S_{cc}(q)$. The response under mechanical constraint is a susceptibility measurement, equivalent to a determination of $\langle u(\mathbf{q})\, u(-\mathbf{q})\rangle$ on account of the fluctuation-dissipation theorem : all these examples illustrate that in the static limit the compressibility modulus which is measured is $\bar{B}$ (at constant chemical potential).

3. Hydrodynamics of two-component smectic A.

The number of relevant hydrodynamic variables to consider can be obtained following the general prescription of MPP [19] by counting the number of conserved quantities and continuously broken symmetries. In the case of the one-component smectic A [18], one hydrodynamic variable associated with the loss of the translational symmetry along the normal to the layers comes into play : the layer displacement u. It adds to the usual five variables of a simple fluid (total mass density ρ, momentum density $\mathbf{g}$, and energy density ε) and that leads to six hydrodynamic modes which are : heat diffusion (corresponding to 1

mode), shear (1), sound (2) and second sound (2). In the case of two-component smectics A [23] we have to take into account one more conserved variable, namely the mass density ρc of a species, and therefore seven modes are present.

The complete mathematical description of these modes, by means of seven coupled hydrodynamic equations, is presented in the appendix. In what follows we set forth a simpler description which rests upon some innocuous approximations. We assume that the system is incompressible and athermal, which amounts to state that the mass density and entropy per unit mass remain at equilibrium. This approximation is valid for any mode with a frequency much smaller than the sound frequency (typically 2 GHz at a wave vector $q = 10^7\ \mathrm{m}^{-1}$) and the thermal mode relaxation frequency (about 1 MHz). It allows the replacement of three hydrodynamic equations by as many *constraints,* on pressure, longitudinal momentum and temperature. Among the four equations that remain, one is uncoupled. It describes a transverse (with respect to both the wave vector and the optical axis), high frequency (about 30 MHz) shear wave. With simplifying (but not essential) assumptions on the symmetry of the viscosity and diffusion coefficient tensors, and on the values of the « flexodiffusion » and permeation dissipative coefficients (taken equal to zero) (see appendix), the remaining three coupled hydrodynamic equations (with a space Fourier transform) are :

$$\begin{aligned}
\partial_t g_t &= -\frac{\eta}{\rho} q^2 g_t - i C_c \frac{q_x q_z}{q} \delta c + (B q_z^2 + K q_x^4) \frac{q_x}{q} u \\
\partial_t \delta c &= -\frac{\alpha_\perp}{\rho^2 \chi} q_x^2 \delta c - i \frac{\alpha_\perp C_c}{\rho^2} q_x^2 q_z u \\
\partial_t u &= -\frac{q_x}{\rho q} g_t .
\end{aligned} \tag{11}$$

In equation (11), the x-z plane contains both the wave vector $\mathbf{q}$ and the normal to the layers (along the z-direction) ; q is the magnitude of $\mathbf{q}$; g_t is a transverse momentum $((q_z g_x - q_x g_z)/q)$; η is a shear viscosity and $\alpha_\perp / \rho^2 \chi$ is the single non-vanishing component of the diffusion coefficient tensor.

These three equations can be solved for arbitrary wave vectors but in order to identify more easily the mode structure we first study limiting cases.

3.1 LIMIT $q_z = 0$. — For $q_z = 0$ equation (11) simplifies and reads :

$$\begin{aligned}
\partial_t g_t &= -\frac{\eta}{\rho} q_x^2 g_t + K q_x^4 u \\
\partial_t \delta c &= -\frac{\alpha_\perp}{\rho^2 \chi} q_x^2 \delta c \\
\partial_t u &= -\frac{g_t}{\rho} .
\end{aligned} \tag{12}$$

In this limit, the concentration fluctuations are decoupled from the layer displacement and transverse momentum ones. Consequently, we recover a one-component smectic A mode structure superimposed to a binary fluid one. The two coupled equations lead to a transverse shear wave and an undulation mode [18, 19]. In the limit $K\rho/\eta^2 \ll 1$, their relaxation frequencies are given by :

$$\omega_s = -i \frac{\eta}{\rho} q_x^2 \qquad \text{(shear mode)} \tag{13a}$$

$$\omega_u = -i \frac{K}{\eta} q_x^2 \qquad \text{(undulation mode)} . \tag{13b}$$

The shear mode is a high-frequency mode (about 30 MHz at $q = 10^7\ \mathrm{m}^{-1}$) that corresponds to $g_t = \eta q_x^2 u$ and $\delta c = 0$: it does not couple to concentration fluctuations and little to layer displacement ones. Consequently, it scatters light very weakly. The undulation mode, with $g_t = K\rho/\eta^2 . \eta q_x^2 . u$ and $\delta c = 0$ is at low frequency (typically 10 kHz), couples strongly to layer displacement fluctuations and is thus easily observable in a light scattering experiment [21, 22] (Fig. 2a shows a schematic representation of this mode). Note that the undulation mode modulates the orientation of the director keeping constant both the intermembrane distance ($q_z = 0$) and the bilayer thickness (since $\delta c = 0$).

The last mode ($g_t = 0, u = 0$) corresponds to concentration fluctuations and therefore to a modulation of the membrane thickness (Fig. 2b). It is reminiscent of the well-known peristaltic mode of soap films [30-33]. Consequently we call it the membrane peristaltic mode. Its dispersion relation is :

$$\omega_p = -i \frac{\alpha_\perp}{\rho^2 \chi} q_x^2 \qquad \text{(membrane peristaltic)} . \tag{13c}$$

The membrane peristaltic mode gives a contribution to light scattering, but its characteristic frequency (about 10 MHz) makes it difficult to observe [24].

3.2 OBLIQUE **q** VECTOR. — For an *oblique* wave vector (i.e. $q_x q_z \neq 0$), the three variables g_t, δc and u are coupled and equation (11) leads to the following three modes [23] : the second sound, which corresponds to two propagative waves ; the *baroclinic* mode, which is diffusive, deserving its name because it corresponds to a *compression* wave at *oblique* **q**.

To lowest order in q, the frequencies of the second sound are given by :

$$\omega_2 = \pm \sqrt{\frac{B}{\rho}} \frac{|q_x q_z|}{q} \qquad \text{(second sound)} . \tag{14a}$$

These frequencies are controlled by B, the layer compressibility modulus at constant concentration and consequently measure mainly the stretching energy of the surfactant bilayer (Eq. (6)).

The relaxation frequency of the baroclinic mode is given, in the limit of small q_x, by :

$$\omega_b = -i \frac{\alpha_\perp}{\rho^2} \frac{\bar{B}}{\chi B} q_x^2 \qquad \text{(baroclinic mode)} . \tag{14b}$$

In contrast to second sound, the relaxation frequency of the baroclinic mode is mainly controlled by membrane interactions, in the dilute range, since $B\chi$ is then of the order of c^2 (see Eq. (6)). In this range, equation (14b) becomes :

$$\omega_b = -i \mu \bar{B} q_x^2, \quad \text{with} \quad \mu = \frac{\alpha_\perp}{\rho^2 c^2} . \tag{15}$$

The baroclinic mode corresponds to $g_t = \rho \mu \bar{B} q q_x u$, $\delta c = -iBq_z u/C_c$ which implies that the layer thickness remains constant ($B/C_c \approx c$ in the dilute range, see Eq. (6)), whereas the layer thickness is strongly modulated by the second sound modes ($\delta c \approx 0$ at non-zero $\partial_z u$). The second sound and the baroclinic modes are schematically shown in figures 2d and 2c respectively. In figure 2 we note that the second sound corresponds to both a variation in the bilayer thickness and in the distance between membranes when the baroclinic mode modulates only the membrane distance and not the bilayer thickness.

The three coupled hydrodynamic equations (Eq. (11)) can of course be solved in the general case to describe the cross-over from $q_z = 0$ to oblique $\mathbf{q}$. The study of the complete solutions for the dispersion relations shows that the undulation and baroclinic modes are on the same branch and therefore two limiting aspects of the same mode. The dispersion relation of the undulation/baroclinic mode displayed in figure 3 illustrates this property. Note that this behaviour has to be compared to the one that obtains in one-component smectic A, where the undulation mode is the limit of the second sound mode at $q_z = 0$. For two-component smectic A phases, the second sound degenerates into the membrane peristaltic mode (this statement corrects a mistake in Ref. [26]). This pecularity of two-component smectic A can be intuitively grasped considering the drawings of figure 2 where it is clear that one limit of the second sound (Fig. 2d) at $q_z = 0$ is the membrane peristaltic mode (Fig. 2b), since these two modes modulate the bilayer thickness, and the limit of the baroclinic mode (Fig. 2c) is the undulation mode (Fig. 2a). In their previous treatment of this problem, Brochard and de Gennes [23] had proposed the same name « slip » for both the membrane peristaltic and baroclinic modes. Since these two modes belong to different branches, we propose to call them by two different names related to their geometrical features (Fig. 2).

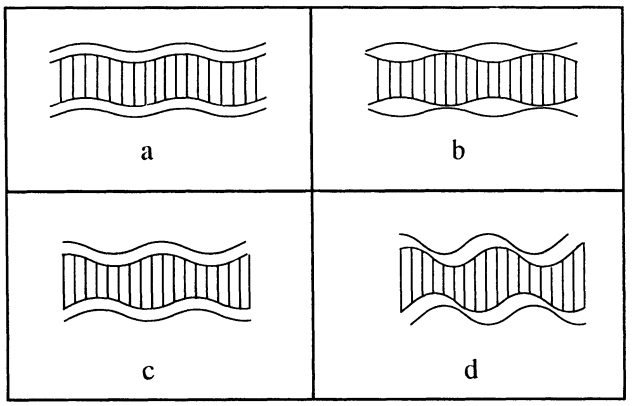

Fig. 2. — Hydrodynamic modes of a two-component smectic A : undulation mode (a) ; membrane peristaltic mode (b) ; baroclinic mode (c) ; second sound mode (d). Modes a and b (respectively c and d) occur for a wave vector parallel to (resp. oblique with respect to) the layers. Mode a (respectively b) continuously merges into mode c (resp. d) as q_z increases from zero.

4. Experimental details.

As made clear by equation (10), only modes coupled to the dielectric tensor can be observed in a light scattering experiment. Such are the membrane peristaltic/second sound and the undulation/baroclinic modes. The first branch is always at high frequencies, therefore our intensity correlation spectroscopy technique will be more sensitive to the undulation/baroclinic branch.

4.1 GEOMETRY OF THE SET UP. — Figure 4 shows the geometry of the set-up we used. The position of the detector is defined by the scattering angle ϕ. Two angles θ and ψ define the direction of the optical axis (oriented samples are used) : the angle θ controls the in-plane rotation (around an axis perpendicular to the scattering plane) and ψ the out-of-plane one

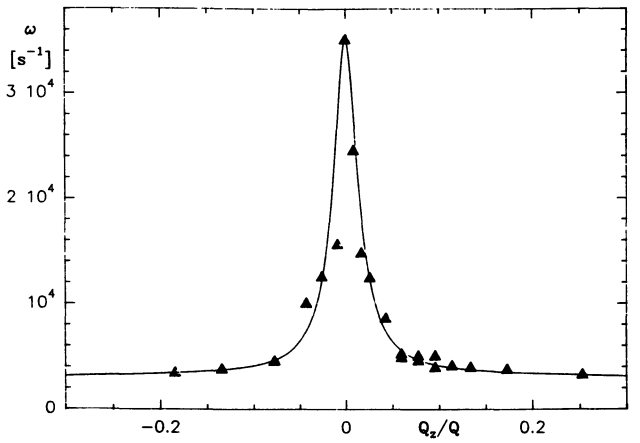

Fig. 3. — Anisotropic dispersion relation of the undulation/baroclinic mode near $q_z = 0$. The smectic bending modulus K is measured from the peak frequency, the compression modulus $\bar{B}$ from the oblique **q** behaviour. The triangles are the experimental data for a sample with $d = 6.1$ nm at $q \approx 1.4 \times 10^7\ \mathrm{m}^{-1}$. The solid line is a theoretical prediction from equation (11).

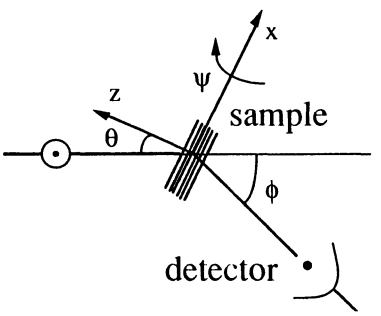

Fig. 4. — Geometry of the set-up, drawn in the scattering plane. The angle ϕ controls the modulus of the wave vector. The z-axis is the projection on the scattering plane of the normal to the layers. The angle ψ controls the out-of-plane orientation of the smectic optical axis. The incident light is always polarized perpendicularly to the scattering plane.

(around an axis parallel to the scattering plane). The incident light is always polarized perpendicularly to the scattering plane (polarization vector **i**). The analyzer is either parallel or perpendicular to the scattering plane (polarization **f**).

Since our sample cells have plane interfaces, in order to compute the magnitude q and the projection q_z of the wave vector, refraction has to be taken into account. We neglect the small optical anisotropy of our samples. With n (resp. n') the index of refraction of the index matching bath (resp. the sample), we get the following expressions for q and q_z :

$$q^2 = \frac{8\pi^2}{\lambda^2}\left(n'^2 - n^2\cos\phi + n^2\cos i\cos f - n'^2\cos i'\cos f'\right)$$
$$q_z = \frac{2\pi n'}{\lambda}\left(\cos i' - \varepsilon\,.\cos f'\right) \qquad (16)$$

with $\cos i = \cos\theta \cos\psi$, $\cos f = \cos(\theta - \phi)\cos\psi$; i' and f' are related to i and f by the Snell-Descartes' law ; ε is $+1$ for θ outside $[\pi/2, \pi/2 + \phi]$ and -1 otherwise. The wavelength in vacuo of the incident light is λ (krypton laser ; $\lambda = 647.1$ nm).

From equation (16) it is clear that the orientation for $q_z = 0$ corresponds to $\theta = \phi/2$ ($i = f$). The choice of this orientation is not sufficient to ensure that one observes the undulation mode : concentration fluctuations are not *coupled* to it (Sect. 3.1) and light scattering selection rules are such that layer displacement fluctuations are not *visible* when $f_z \mathbf{i} \cdot \mathbf{q}_\perp + i_z \mathbf{f} \cdot \mathbf{q}_\perp$ is equal to zero (Eq. (10)). To observe the undulation mode one thus has to choose $\psi \neq 0$ and polarizer and analyzer at right angles.

4.2 SAMPLE PREPARATION. — We studied a series of samples corresponding to quaternary water/sodium dodecylsulphate/pentanol/dodecane systems. The phase diagram of this system at constant temperature (21 °C) is known in detail [34] and high resolution X-ray [14] and mechanical [13] techniques have been used to measure quantities related to the elastic constants $\bar{B}$ and K. A short report of preliminary results on $\bar{B}$ has been given in a previous letter [26]. Starting with a concentrated sample (no dodecane) in the lamellar phase it is possible to swell the membranes with a mixture of dodecane and pentanol. The bilayers are 19 Å thick and can be swollen continuously from a repeating distance d of 35 Å to 400 Å (for a given water over surfactant mass ratio of 1.55). The samples once prepared are put in rectangular glass capillaries (100 μm thick, 1 mm wide and 30 mm long) which are then sealed. A good homeotropic orientation is achieved using a thermal treatment : the samples are heated up to the lamellar-isotropic phase transition then slowly cooled down to room temperature (cooling rate about 0.1 °C min^{-1}).

5. Results.

Experiments have been performed for three values of the angle ψ : $\psi = 0°$, $\psi = 25°$ and $\psi = 70°$. At $\psi = 0°$ and when $q_z = 0$, concentration fluctuations alone can be detected (Eq. (10)). The only mode that could be seen in this case is the membrane peristaltic mode. As discussed previously, it is not readily observable in our experiment. Indeed, for $\psi = 0°$ and $q_z = 0$ the recorded signal is very weak, usually not monoexponential and poorly reproducible. It originates probably in the small remaining unoriented parts of the sample (which are not at $q_z = 0$). Away from $q_z = 0$, we pick up a nice, monoexponential and polarized signal which corresponds then to the baroclinic/undulation branch. When $\psi = 25°$ or $\psi = 70°$ we clearly follow the same branch for oblique $\mathbf{q}$ but now near $q_z = 0$ we get a significant monoexponential depolarized signal corresponding to the pure undulation mode (Fig. 3).

5.1 UNDULATION MODE. — The experimental dispersion relation of the undulation mode is obtained according to the following procedure : with $\psi = 25°$ (or $\psi = 70°$), at a given angle ϕ, polarizers being crossed, we record a relaxation frequency varying the angle θ in the vicinity of $\phi/2$: this varies the projection q_z around zero at fixed modulus of the wave vector $\mathbf{q}$. The maximum relaxation frequency, which occurs at $q_z = 0$, allows us to accurately determine the undulation mode frequency. The sharpness of this maximum can be appreciated in figure 3. Repeating this procedure for different angles ϕ (i.e. different values of q), we determine the dispersion curve ω_u as a function of q. The angles ϕ lie in the range 10°-90°. Figure 5 shows typical data for two samples at different dilutions ($d = 113$ Å and $d = 344$ Å). As expected from the theory (Eq. (13b)) we get ω_u proportional to the square of q. The proportionality constant D_u is the ratio of the smectic bending modulus K to the viscosity η. The resulting values of $1/D_u$ (i.e. η/K) as a function of the repeating distances d are plotted figure 6.

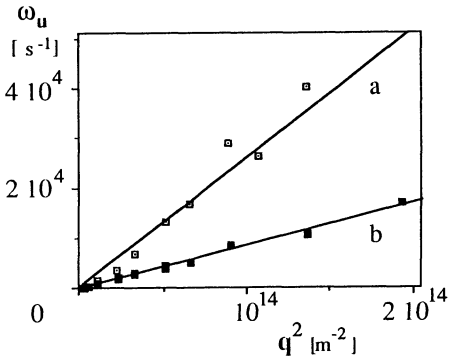

Fig. 5. — Undulation mode dispersion relation at different dilutions ; d = 11.3 nm (a) and d = 34.4 nm (b).

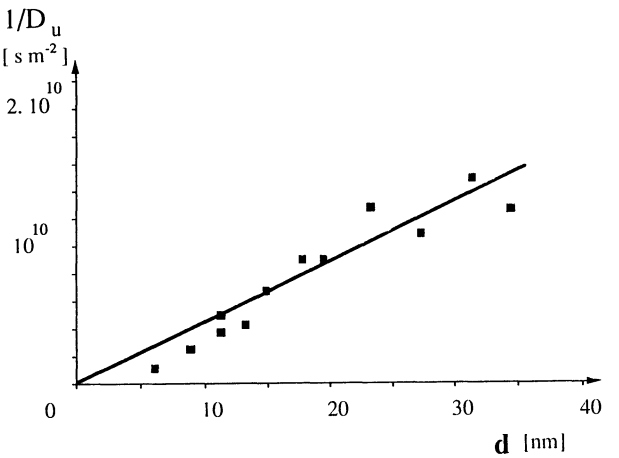

Fig. 6. — Inverse slope $1/D_u$ of the undulation mode dispersion relation as a function of the smectic repeating distance d. Filled squares : experimental data ; solid line : prediction from equation (18), with $\kappa = 0.8\, k_B\, T$.

5.2 BAROCLINIC MODE. — The experimental dispersion relation of the baroclinic mode obtains according to one of the two following procedures : i) at $\psi = 0°$ and ϕ fixed, without analyzing the polarization of the scattered light, we record the relaxation frequency as a function of θ, scanning the entire range $\phi/2 \leq \theta \leq \phi/2 + \pi/2$. There is no relevant signal close to the limit $\theta = \phi/2$ ($q_z = 0$) as explained above, nor close to the limit $\theta = \phi/2 + \pi/2$ because of the specular reflection by the capillary of the incident light into the detector ; ii) at $\psi = 25°$ (or $\psi = 70°$) and ϕ fixed, we again scan the entire range $\phi/2 \leq \phi \leq \theta/2 + \pi/2$, the polarizers being crossed (θ in the vicinity of $\phi/2$), or parallel. In this case we are able to record a signal at any θ, but are restricted in the q_z range since its maximum value (at $\theta = \phi/2 + \pi/2$) is now $q \cos \psi$ instead of q. Note that the experimental points of figure 3 have been obtained following this second procedure. For each procedure we then vary the angle ϕ between 15° and 160°. We checked that they gave equivalent results. Figure 7 displays representative data for the relaxation frequency ω_b of the baroclinic mode for two different

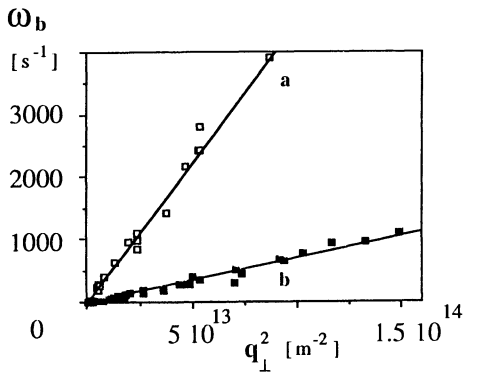

Fig. 7. — Baroclinic mode dispersion relation at different dilutions ; $d = 6.1$ nm (a) and $d = 23.2$ nm (b).

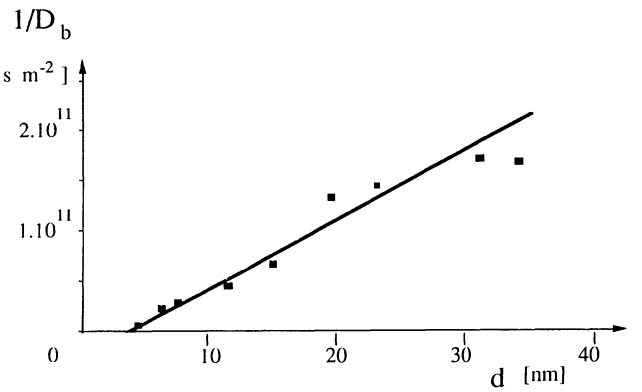

Fig. 8. — Inverse slope $1/D_b$ of the baroclinic mode dispersion relation as a function of the smectic repeating distance d. Filled squares : experimental data ; solid line : prediction from equation (21) with $\kappa = 2.4\, k_B\, T$.

samples (repeating distances $d = 60.8$ Å and $d = 232$ Å), as a function of the square of $q_\perp$ ($q_\perp^2 = q^2 - q_z^2$), far from the $q_z = 0$ limit. In this range the dispersion relation is linear in $q_\perp^2$, in accordance to the theoretical prediction of equation (14b). The inverse slope $1/D_b$, which is the inverse of the smectic compression modulus at constant chemical potential $\bar{B}$, divided by the mobility μ, is plotted as a function of the repeating distance d figure 8.

6. Discussion.

In order to interpret the behaviour under dilution of the « diffusion coefficients » D_u and D_b, we need to introduce a microscopic calculation for the friction parameters μ and η and to model the d-dependence of K and $\bar{B}$.

6.1 MICROSCOPIC MODEL FOR THE DISSIPATIVE COEFFICIENTS. — Following Brochard and de Gennes [23], we assume that η is the pure solvent viscosity η_S (dodecane ; $\eta_S = 1.35 \times 10^{-3}$ Pa.s). This is probably realistic for very dilute samples even though the case

of concentrated ones is less obvious. As regards μ, we first notice that it appears in both relaxation frequencies of the membrane peristaltic and baroclinic modes (compare Eq. (13c) and Eq. (15)) and then again refer to Brochard and de Gennes [23], who calculated μ for the membrane-peristaltic mode from the solvent Poiseuille flow, to get :

$$\mu = \frac{\beta (d - \delta)^2}{12\, \eta_S} \tag{17}$$

with $\beta (d) = \dfrac{\rho_S\, d}{\rho_S (d - \delta) + \rho_M\, \delta}$ and ρ_S (resp. ρ_M) the mass density of the solvent (resp. the membrane).

6.2 ELASTIC CONSTANTS. — The elastic constants K and $\bar{B}$ can be modelled using the description of a lyotropic smectic phase as a stack of interacting membranes. The layer bending modulus K reflects the membrane flexibility : since the smectic A phase is built from a stack of membranes that remain essentially identical upon dilution we expect $K = \kappa/d$, where κ is the *membrane* bending modulus. Therefore, we get the dilution dependence for D_u :

$$D_u = \frac{\kappa}{\eta_S} \frac{1}{d}\,. \tag{18}$$

The least square fit using equation (18) is shown in figure 6 which yields a value of $\kappa = 0.8\, k_B\, T$. On the dilution range investigated the experimental bending modulus K decreases continuously from about 4×10^{-13} N to 1×10^{-13} N which is about two orders of magnitude smaller than values commonly encountered in thermotropic smectics A ($K \approx 10^{-11}$ N). Note that this is partly caused by the intrinsic large flexibility (low κ) of the membrane and partly by the dependence on d (« colloidal effect »).

The layer compression modulus $\bar{B}$ is directly related to the intermembrane interactions (Eq. (7)). For the system we study, previous experiments [14, 15] have shown that the relevant interactions come from the hindrance to thermally excited undulations originating in the steric short range repulsion between membranes. These are Helfrich's undulation forces [8]. In the smectic case, the resulting interaction potential per unit area is [8, 11] :

$$V(d) = \frac{3\, \pi^2 k_B\, T}{128} \frac{k_B\, T}{\kappa} \frac{}{(d - \delta)^2}\,. \tag{19}$$

With equations (7) and (19) we get :

$$\bar{B} = \frac{9\, \pi^2}{64} \frac{(k_B\, T)^2}{\kappa} \frac{d}{(d - \delta)^4} \tag{20}$$

and thus (Eqs. (17) and (20)) :

$$D_b = \frac{3\, \pi^2 \beta}{256\, \eta_S} \frac{(k_B\, T)^2}{\kappa} \frac{d}{(d - \delta)^2}\,. \tag{21}$$

The solid line in figure 8 corresponds to a fit using equation (21) with only one adjustable parameter, namely κ (the membrane thickness δ being fixed to 30 Å [14]). The result is $\kappa = 2.4\, k_B\, T$. The layer compression modulus $\bar{B}$ ranges from 5×10^4 Pa to 10^2 Pa which is

about two to six orders of magnitude less than a typical thermotropic value. This effect comes mainly from the large value of the repeating distance $d(\bar{B} \propto d^{-3})$.

7. Conclusion.

We have shown that light scattering techniques allow in principle to have an access to *all* the elastic coefficients of the lyotropic smectic A free energy. This can be performed with the selection of both the polarizations and the wave vector **q**. The velocity of the propagative second sound mode at oblique **q** is a measure of the layer compressibility modulus at constant concentration (B) ; the relaxation frequency of the limiting membrane peristaltic mode $(q_z = 0)$ gives the osmotic compressibility at constant layer spacing (χ). The baroclinic mode at oblique **q** vector has a relaxation frequency proportional to the layer compressibility at constant chemical potential $(\bar{B})$; its limiting behaviour at $q_z = 0$ (the undulation mode) depends on the bending modulus (K). We have noted the difference between thermotropic (one-component) smectics A and lyotropic (two-component) ones : namely, the second sound branch contains the undulation mode in the thermotropic case whereas for lyotropic systems it degenerates into the membrane peristaltic mode ; the baroclinic mode then leads to the undulation mode in the limit $q_z = 0$.

In these series of experiments we have presented results for the baroclinic/undulation branch and checked the dispersion relation including the crossover regime. We did not present results for the second sound/membrane peristaltic mode mainly because it is at much higher frequencies and gives a weak signal. In principle this other branch could be observed at small q (smaller frequencies). Another interesting development of this work would be to measure the static light scattering intensities that are also related to the elastic constants.

The study of the baroclinic/undulation mode allows us to measure K and $\bar{B}$ for a dilute lamellar phase along a dilution line. We have *directly* measured the elastic constant K and checked that it behaves as $1/d$, the membrane bending modulus being $\kappa = 0.8\, k_B\, T$. This confirms that this system is very flexible [14, 26]. Moreover, we have measured the interactions between membranes and established the d^{-3} dependence for $\bar{B}$, coming from the undulation forces. The magnitude of the undulation forces is a function of the bending modulus κ, therefore we can also extract its value from the $\bar{B}$ measurements : we found $\kappa = 2.4\, k_B\, T$. This is comparable (but not equal) to what we got from the undulation mode study. This difference by a factor 3 is unimportant at the present stage of understanding of the dissipative coefficients μ and η [36].

Acknowledgements.

The authors are very grateful to Scott Milner for extensive discussions and correspondence concerning the physical interpretation of the hydrodynamic modes ; they thank Tom Lubensky and Sriram Ramaswamy for their comments on the microscopic model ; they also would like to acknowledge discussions with Grégoire Porte and Patricia Bassereau on many aspects of this work.

Appendix.

We detail here the hydrodynamic properties of a two-component smectic A phase. The seven independent hydrodynamic variables to consider are [19, 23] : total mass density ρ, momentum density **g**, energy density ε, as in any simple fluid ; mass density ρc of a species

(two-component system) and layer displacement u (smectic A system). The evolution in time of these variables is described by :

$$\begin{aligned} \partial_t \rho &= -\nabla \cdot \mathbf{g} \\ \partial_t g_i &= -\partial_j \sigma_{ij} \ (i = x, y \text{ or } z) \\ \partial_t \varepsilon &= -\nabla \cdot \mathbf{J}_\varepsilon \\ \partial_t (\rho c) &= -\nabla \cdot \mathbf{J}_c \\ \partial_t u &= J_u \, . \end{aligned} \tag{A.1}$$

The first six equations are the conservation laws, stated on a local form, for the corresponding conserved variables. The mass flux is the momentum density ; the momentum flux is the stress tensor σ_{ij} ; $\mathbf{J}_\varepsilon(\mathbf{J}_c)$ is the energy (particle) current density. The last equation is *not* a continuity equation since u is *not* a conserved variable ; J_u describes the relaxation of u towards equilibrium.

To close this set of equations, the fluxes σ_{ij}, $\mathbf{J}_\varepsilon$, $\mathbf{J}_c$ and J_u must be known. The thermodynamic and symmetry properties of the system (with the usual assumptions of local equilibrium and monotonic increase of entropy with time) set general constraints upon the fluxes that allow to state them more explicitly. Following the general MPP derivation [19], care duly taken that the two extra hydrodynamic variables are not on the same footing since ρc is a conserved variable whereas u is a broken-symmetry one, we get :

$$\begin{aligned} \sigma_{ij} &= p \delta_{ij} - \Phi_j \, \delta_{iz} + \sigma_{ij}^{\mathrm{D}} \\ \mathbf{J}_\varepsilon &= \frac{p + \varepsilon}{\rho} \mathbf{g} + \mathbf{J}_\varepsilon^{\mathrm{D}} \\ \mathbf{J}_c &= c\mathbf{g} + \mathbf{J}_c^{\mathrm{D}} \\ J_u &= \frac{g_z}{\rho} + J_u^{\mathrm{D}} \end{aligned} \tag{A.2}$$

(the z-direction of the coordinate axes is perpendicular to the smectic layers). In these equations the terms with a D superscript are the *dissipative* contributions to the fluxes : if all D-terms are set equal to zero the total entropy remains constant. The other terms are the so-called *reactive* fluxes. As in the one-component smectic A case, there is a twofold contribution to the reactive part of the stress tensor : the first is the pressure p ; the second comes from the « stress vector » $\mathbf{\Phi}$ which describes the elastic response to a strain u. The dissipative fluxes are given by the following constitutive relations :

$$\begin{aligned} J_{ci}^{\mathrm{D}} &= -(\alpha_\perp \, \partial_i \tilde{\mu} + (\alpha_z - \alpha_\perp) \, \partial_z \tilde{\mu} \, \delta_{iz}) - (\beta_\perp \, \partial_i T + (\beta_z - \beta_\perp) \, \partial_z T \, \delta_{iz}) - \Gamma \, \delta_{iz} \nabla \cdot \mathbf{\Phi} \\ J_{\varepsilon i}^{\mathrm{D}} &= \tilde{\mu} J_{ci}^{\mathrm{D}} - (\kappa_\perp \, \partial_i T + (\kappa_z - \kappa_\perp) \, \partial_z T \, \delta_{iz}) - T(\beta_\perp \, \partial_i \tilde{\mu} + (\beta_z - \beta_\perp) \, \partial_z \tilde{\mu} \, \delta_{iz}) - \xi \, \delta_{iz} \nabla \cdot \mathbf{\Phi} \\ J_u^{\mathrm{D}} &= \frac{\xi}{T} \partial_z T + \Gamma \, \partial_z \tilde{\mu} + \zeta \nabla \cdot \mathbf{\Phi} \\ \sigma_{ij}^{\mathrm{D}} &= -\eta_{ijk\ell} \, \partial_k (g_1/\rho) \, . \end{aligned} \tag{A.3}$$

In these equations, T stands for the absolute temperature and $\tilde{\mu}$ is the difference between the chemical potentials (per unit mass) for the two species. The dissipative coefficients describe mass diffusion (α_z, $\alpha_\perp$), heat diffusion (κ_z, $\kappa_\perp$), permeation (ζ) [35], viscous dissipation ($\eta_{ijk\ell}$: five independent viscosities, explicitly given by Martin *et al.* [19]) and cross-processes : thermodiffusion (β_z, $\beta_\perp$), « thermoflexion » or coupling between heat diffusion and layer displacement (ξ ; already present in the one-component smectic A case)

and « flexodiffusion » or coupling between mass diffusion and layer displacement (Γ ; specific to the two-component smectic A case).

After replacement of the dissipative fluxes by their expressions (Eq. (A.3)) the (linearized) hydrodynamic equations now read :

$$\begin{aligned}
\partial_t \rho &= -\nabla \cdot \mathbf{g} \\
\partial_t g_i &= -\partial_i p + \delta_{iz} \nabla \cdot \mathbf{\Phi} + \eta_{ijk\ell}\, \partial_{jk}(g_\ell/\rho) \\
\rho T\, \partial_t s &= \kappa_\perp \nabla_\perp^2 T + \kappa_z\, \partial_{zz} T + T(\beta_\perp \nabla_\perp^2 \tilde{\mu} + \beta_z\, \partial_{zz} \tilde{\mu}) + \xi\, \partial_z \nabla \cdot \mathbf{\Phi} \\
\rho\, \partial_t c &= \alpha_\perp \nabla_\perp^2 \tilde{\mu} + \alpha_z\, \partial_{zz} \tilde{\mu} + \beta_\perp \nabla_\perp^2 T + \beta_z\, \partial_{zz} T + \Gamma\, \partial_z \nabla \cdot \mathbf{\Phi} \\
\partial_t u &= \frac{g_z}{\rho} + \frac{\xi}{T} \partial_z T + \Gamma\, \partial_z \tilde{\mu} + \zeta\, \nabla \cdot \mathbf{\Phi}
\end{aligned} \tag{A.4}$$

where we have used instead of the energy density ε the entropy per unit mass s. Pressure p, temperature T, chemical potential difference $\tilde{\mu}$ and stress vector $\mathbf{\Phi}$ are still to be expressed in terms of mass density ρ, entropy s, mass fraction c and strain u, with the help of the thermodynamic relation (up to second order) :

$$\begin{aligned}
\delta\left(\frac{\varepsilon}{\rho}\right) &= T\, \delta s + \frac{p}{\rho^2}\, \delta\rho + \tilde{\mu}\, \delta c + \\
&+ \frac{1}{2}\left\{ \frac{B}{\rho} (\partial_z u)^2 + \frac{K}{\rho} (\nabla_\perp^2 u)^2 + \frac{\rho T}{c_V}\, \delta s^2 + \frac{\partial}{\partial \rho}\left(\frac{p}{\rho^2}\right) \delta\rho^2 + \frac{\partial \tilde{\mu}}{\partial c}\, \delta c^2 \right\} + \\
&+ \frac{C_s}{\rho} \partial_z u\, \delta s + \frac{C_\rho}{\rho} \partial_z u\, \delta\rho + \frac{C_c}{\rho} \partial_z u\, \delta c + \frac{\partial T}{\partial \rho}\, \delta s\, \delta\rho + \frac{\partial T}{\partial c}\, \delta s\, \delta c + \frac{1}{\rho^2} \frac{\partial p}{\partial c}\, \delta\rho\, \delta c\,.
\end{aligned} \tag{A.5}$$

The notations are : layer compressibility modulus at constant entropy, mass density and composition : B ; layer curvature modulus : K ; heat capacity at constant density and composition, per unit volume of an unstrained smectic : c_V ; crossed coefficients : C_s, C_ρ and C_c (this last one specific to the two-component smectic A case). With the definitions :

$$p = \rho^2 \left(\frac{\partial(\varepsilon/\rho)}{\partial \rho} \right)_{s,c,u}, \quad T = \frac{1}{\rho} \left(\frac{\partial \varepsilon}{\partial s} \right)_{\rho,c,u}, \quad \tilde{\mu} = \frac{1}{\rho} \left(\frac{\partial \varepsilon}{\partial c} \right)_{s,\rho,u}$$

and

$$\partial_i \Phi_i = -\left(\frac{\delta \varepsilon}{\delta u} \right)_{s,\rho,c}$$

we have for small departures from equilibrium :

$$\begin{aligned}
\delta p &= \rho C_\rho\, \partial_z u + \frac{\partial p}{\partial c}\, \delta c + \rho^2 \frac{\partial(p/\rho^2)}{\partial \rho}\, \delta\rho + \rho^2 \frac{\partial T}{\partial \rho}\, \delta s \\
\delta \tilde{\mu} &= \frac{C_c}{\rho} \partial_z u + \frac{\partial \tilde{\mu}}{\partial c}\, \delta c + \frac{1}{\rho^2} \frac{\partial p}{\partial c}\, \delta\rho + \frac{\partial T}{\partial c}\, \delta s \\
\delta T &= \frac{C_s}{\rho} \partial_z u + \frac{\partial T}{\partial c}\, \delta c + \frac{\partial T}{\partial \rho}\, \delta\rho + \frac{\rho T}{c_V}\, \delta s \\
\mathbf{\Phi}_z &= B\, \partial_z u + C_c\, \delta c + C_\rho\, \delta\rho + C_s\, \delta s \\
\mathbf{\Phi}_i &= -K\, \partial_i \nabla_\perp^2 \mathrm{u} \quad (i = x, y)\,.
\end{aligned} \tag{A.6}$$

The general solution of the complete set of hydrodynamic equations (Eqs. (A.4) and (A.6)) will not be attempted here. We shall rather restrict our analysis to the case where the compressibility and the heat capacity are small : then mass density and entropy per unit mass remain very close to equilibrium and $\delta\rho \cong 0$ and $\delta s \cong 0$. Within the scope of this approximation, pressure, a component of the momentum and temperature are not independent hydrodynamic variables. They are on the contrary *constrained* by the hydrodynamic equations themselves. To proceed further, we resort to Fourier transform in space. With coordinate axes such that the x-z plane contains both the wave vector $\mathbf{q}$ and the normal to the layers ($q_y = 0$) we get the constraints :

$$\begin{aligned} \delta p &= \frac{q_z}{q^2}\,\mathbf{q}\cdot\mathbf{\Phi} + i\,\frac{q_x\,q_z}{q^2}\,\frac{\tilde{\eta}_\ell(\mathbf{q})}{\rho}\,g_t \\ \delta T &= -\,T\,\frac{\beta_\perp\,q_x^2 + \beta_z\,q_z^2}{\kappa_\perp\,q_x^2 + \kappa_z\,q_z^2}\,\delta\tilde{\mu} - \frac{\xi q_z}{\kappa_\perp\,q_x^2 + \kappa_z\,q_z^2}\,\mathbf{q}\cdot\mathbf{\Phi} \\ g_\ell &= 0 \end{aligned} \tag{A.7}$$

and the dynamical equations :

$$\begin{aligned} \partial_t g_y &= -\,\frac{\tilde{\eta}_y(\mathbf{q})}{\rho}\,q^2 g_y \\ \partial_t g_t &= -\,\frac{\tilde{\eta}_t(\mathbf{q})}{\rho}\,q^2 g_t - i\,\frac{q_x}{q}\,\mathbf{q}\cdot\mathbf{\Phi} \\ \partial_t c &= -\,\frac{\tilde{\alpha}(\mathbf{q})}{\rho}\,q^2\,\delta\tilde{\mu} - \frac{\tilde{\Gamma}(\mathbf{q})}{\rho}\,q_z\,\mathbf{q}\cdot\mathbf{\Phi} \\ \partial_t u &= -\,\frac{q_x}{\rho q}\,g_t + i\,\tilde{\Gamma}(\mathbf{q})\,q_z\,\delta\tilde{\mu} + i\,\tilde{\zeta}\mathbf{q}\cdot\mathbf{\Phi} \end{aligned} \tag{A.8}$$

where we introduced the new variables :

$$\begin{aligned} g_\ell &= (q_x g_x + q_z g_z)/q \\ g_t &= (q_z g_x - q_x g_z)/q \end{aligned}$$

and effective dissipative coefficients :

$$\begin{aligned} \tilde{\eta}_t(\mathbf{q}) &= \frac{\eta_3\,q_z^4 + (\eta_1 + \eta_2 + \eta_4 - 2\,\eta_3 - 2\,\eta_5)\,q_x^2 q_z^2 + \eta_3\,q_x^4}{q^4} \\ \tilde{\eta}_\ell(\mathbf{q}) &= \frac{(2\,\eta_3 + \eta_5 - \eta_1)\,q_z^2 + (\eta_2 + \eta_4 - \eta_5 - 2\,\eta_3)\,q_x^2}{q^2} \\ \tilde{\eta}_y(\mathbf{q}) &= \frac{\eta_3\,q_z^2 + \eta_2\,q_x^2}{q^2} \\ \tilde{\alpha}(\mathbf{q}) &= \frac{\alpha_\perp\,q_x^2 + \alpha_z\,q_z^2 - T\,\dfrac{(\beta_\perp\,q_x^2 + \beta_z\,q_z^2)^2}{\kappa_\perp\,q_x^2 + \kappa_z\,q_z^2}}{q^2} \\ \tilde{\Gamma}(\mathbf{q}) &= \Gamma - \frac{\beta_\perp\,q_x^2 + \beta_z\,q_z^2}{\kappa_\perp\,q_x^2 + \kappa_z\,q_z^2}\,\xi \\ \tilde{\zeta}(\mathbf{q}) &= \zeta - \frac{\xi^2 q_z^2}{T(\kappa_\perp\,q_x^2 + \kappa_z\,q_z^2)}\,. \end{aligned} \tag{A.9}$$

The relevant hydrodynamic equations can now be written as a matrix equation : $\partial_t X = M \cdot X$, with X, the column vector $(g_t, \delta c, u)$ and M, the three-by-three matrix given below :

$$\begin{bmatrix} -\frac{\tilde{\eta}_t}{\rho} q^2 & -iC_c \frac{q_x q_z}{q} & +(Bq_z^2 + q_x^4)\frac{q_x}{q} \\ 0 & -\frac{\tilde{\alpha}\frac{\partial\tilde{\mu}}{\partial c} q^2 + \tilde{\Gamma} C_c q_z^2}{\rho} & -i\frac{\tilde{\Gamma}(Bq_z^2 + Kq_x^4)\rho + \tilde{\alpha} C_c q^2}{\rho^2} q_z \\ -\frac{q_x}{\rho q} & i\left(\tilde{\Gamma}\frac{\partial\tilde{\mu}}{\partial c} + \tilde{\zeta} C_c\right) q_z & -\left\{\frac{\tilde{\Gamma} C_c}{\rho} q_z^2 + \tilde{\zeta}(Bq_z^2 + Kq_x^4)\right\} \end{bmatrix}.$$

The hydrodynamic mode structure follows from the properties of this matrix : its eigenvectors are the hydrodynamic modes ; they relax towards equilibrium with frequencies given by its eigenvalues. At the leading order in a wave vector expansion, a real eigenvalue (i.e. a pure imaginary frequency) corresponds to a *diffusive* mode and a pure imaginary one to a *propagative* mode. The hydrodynamic equations given in the main text (Eq. (11)) result from a simplification of the matrix coefficients :

$\tilde{\eta}_t(\mathbf{q}) = \eta$ (viscosity tensor $\eta_{ijk\ell}$ reduced to its isotropic limit)

$\tilde{\alpha}(\mathbf{q}) = \alpha_\perp \frac{q_x^2}{q^2}$ (no particle diffusion, heat diffusion or thermodiffusion along the z direction)

$\tilde{\Gamma}(\mathbf{q})$ and $\tilde{\zeta}(\mathbf{q})$ equal to zero. (Permeation ; coupling between heat or particle diffusion with layer displacement neglected),

with the notation $\chi^{-1} = \rho\,(\partial\mu/\partial c)$. These simplifications do not affect *qualitatively* the mode structure discussed in the text. The limit $q_x = 0$ is *quantitatively* modified, however : instead of being a zero frequency mode at $q_x = 0$, as follows from equation (14b), the baroclinic mode (which becomes in this limit the permeation mode) is at the (expected small) frequency $\omega_{\text{perm.}}$:

$$\omega_{\text{perm.}} \cong -i\left(\tilde{\zeta} - \frac{\tilde{\Gamma}}{\tilde{\alpha}}\right) \bar{B} q_z^2 \qquad \text{(permeation mode)}\,. \tag{A.10}$$

Similarly, the limiting frequencies of the second sound are actually finite. One of them is associated to the (slow) mode that corresponds to the diffusion of one species normally to the layers $(\delta c \neq 0, g_t = 0, u = 0)$:

$$\omega_d \cong -i\frac{\tilde{\alpha}}{\rho^2 \chi} q_z^2\,. \tag{A.11}$$

The second one is the (high) relaxation frequency of a transverse shear wave.

References

[1] EKWALL P., Advances in Liquid Crystals, G. M. Brown Ed. (Academic, New York) 1975.

[2] BENTON W. J. and MILLER C. A., *J. Phys. Chem.* **87** (1983) 4981.

[3] DVOLAITZKY M., OBER R., BILLARD J., TAUPIN C., CHARVOLIN J. and HENDRIX Y., *C. R. Hebd. Acad. Sci. Paris* **II 45** (1981) 295.

[4] BELLOCQ A.-M. and ROUX D., Microemulsions, Frieberg and Bothorel Eds. (CRC Press) 1986.

[5] LARCHÉ F., APPELL J., PORTE G., BASSEREAU P. and MARIGNAN J., *Phys. Rev. Lett.* **56** (1986) 1700.

[6] LICHTERFELD F., SCHMELING T. and STREY R., *J. Phys. Chem.* **90** (1986) 5762.

[7] SATOH N. and TSUJII K., *J. Phys. Chem.* **91** (1987) 6629.

[8] HELFRICH W., *Z. Naturforsch.* **33a** (1978) 305.

[9] HELFRICH W., *J. Phys. France* **46** (1985) 1263.

[10] PELITI L. and LEIBLER S., *Phys. Rev. Lett.* **54** (1985) 1690.

[11] LEIBLER S. and LIPLOWSKI R., *Phys. Rev.* **B 35** (1987) 7004.

[12] DI MÉGLIO J.-M., DVOLAITZKY M. and TAUPIN C., *J. Phys. Chem.* **89** (1985) 871.

[13] NALLET F. and PROST J., *Europhys. Lett.* **4** (1987) 307.

[14] SAFINYA C. R., ROUX D., SMITH G. S., SINHA S. K., DIMON P., CLARK N. A. and BELLOCQ A.-M., *Phys. Rev. Lett.* **57** (1986) 2718.

[15] ROUX D. and SAFINYA C. R., *J. Phys. France* **49** (1988) 307.

[16] DE GENNES P.-G., Scaling concepts in polymer physics (Cornell university press) 1979.

[17] FISHER M. E. and FISHER D. S., *Phys. Rev.* **B 25** (1982) 3192.

[18] DE GENNES P.-G., *J. Phys. France* **30** (1969) C-65.

[19] MARTIN P. C., PARODI O. and PERSHAN P. S., *Phys. Rev.* **A 6** (1972) 2401.

[20] LIAO Y., CLARK N. A. and PERSHAN P. S., *Phys. Rev. Lett.* **30** (1973) 639.

[21] RIBOTTA R., SALIN R. and DURAND G., *Phys. Rev. Lett.* **32** (1974) 6.

[22] BIRECKI H., SCHAETZING R., RONDELEZ F. and LITSTER J. D., *Phys. Rev. Lett.* **36** (1976) 1376.

[23] BROCHARD F. and DE GENNES P.-G., *Pramana Suppl.* **1** (1975) 1.

[24] CHAN W. and PERSHAN P. S., *Phys. Rev. Lett.* **39** (1977) 1368.

[25] DI MÉGLIO J.-M., DVOLAITSKY M., LÉGER L. and TAUPIN C., *Phys. Rev. Lett.* **54** (1985) 1686.

[26] NALLET F., ROUX D. and PROST J., *Phys. Rev. Lett.* **62** (1989) 276.

[27] The above geometrical description is not a *realistic* microscopic model of dilute lamellar phases : the fluctuation-induced crumpling of the surfactant membrane must be taken into account. A more careful treatment (Lubensky T. C., Prost J., Ramaswamy S., unpublished) results in a dilution behaviour different from the prediction of equation (6). However, the inequality $\bar{B} \ll B$ obtains. Besides, the link between B (or χ) and membrane stretching, or between $\bar{B}$ and membrane interactions, suggested by figure 1, still holds.

[28] CAILLÉ A., *C.R. Hebd. Acad. Sci. Paris* **B 274** (1972) 891.

[29] PORTE G., MARIGNAN J., BASSEREAU P., MAY R., *Europhys. Lett.* **7** (1988) 713.

[30] VRIJ A., *Adv. Colloid Interface Sci.* **2** (1968) 39.

[31] LUCASSEN K., VAN DEN TEMPEL M., VRIJ A. and HESSELINK F. T., *Proc. K. Ned. Akad. Wet.* **B 73** (1970) 109.

[32] VRIJ A., HESSELINK F. T., LUCASSEN J. and VAN DEN TEMPEL M., *Proc. K. Ned. Akad. Wet.* **B 73** (1970) 124.

[33] YOUNG C. Y. and CLARK N. A., *J. Chem. Phys.* **74** (1981) 4171.

[34] ROUX D. and BELLOCQ A.-M., Physics of Amphiphiles, V. Degiorgio and M. Corti Eds. (North-Holland, Amsterdam) 1985.

[35] HELFRICH W., *Phys. Rev. Lett.* **23** (1969) 372.

[36] Another possible explanation could be the renormalization of κ by thermal fluctuations [9, 10]. Although reducing the difference (factor 2 instead of 3), this effect is not enough to bridge the gap between the two values.